

Design and manufacture of krypton gas target for ^{81}Rb production at a 30 MeV cyclotron

M. R. Aboudzadeh Rovais,
 Mohammad Mirzaii,
 Mohsen Kiyomarsi,
 Kamran Yousefi,
 Nami Shadanpour,
 Mohammad R. Ensaf

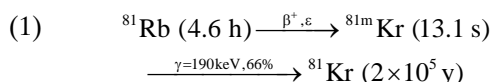
Abstract. The cyclotron of nuclear medicine research group at the Agricultural, Medical and Industrial Research School (AMIRS) has been producing several radionuclides such as ^{201}Tl , ^{67}Ga , ^{18}F and ^{81}Rb for nuclear medicine centers. Gas targets are utilized in a variety of cyclotron producing radionuclides which are used in nuclear medicine centers. We report a method for the design and manufacture of a cyclotron gas target which facilitates both the collection and processing of the krypton gas target as well as the desired ^{81}Rb . In this study a gas target was designed for routine production of ^{81}Rb (for a $^{81}\text{Rb}/^{81\text{m}}\text{Kr}$ generator) through the nuclear reaction $^{nat}\text{Kr}(p,2n)^{81}\text{Rb} \rightarrow ^{81\text{m}}\text{Kr}$. The incident energy of protons on the target was 26.5 MeV. The gas target was made of stainless steel. The length of the target was 251 mm with double titanium windows, 20 μm in thickness. A production yield of 3.18 ± 0.27 mCi/ $\mu\text{A}\cdot\text{h}$ was obtained which was more than 80% of the calculated yield (4.1 mCi/ $\mu\text{A}\cdot\text{h}$).

Key words: targetry • cross-section • yield • ^{81}Rb • gas target • Monte Carlo simulator

Introduction

Cyclotron produced radionuclides have diagnostic applications in nuclear medicine. Production of these radionuclides is supported from the field of nuclear data, targetry, chemical processing, automation and quality control. In the past decades there has been a significant increase in the interest of nuclear medicine departments for the utilization of short-lived radionuclides and radiopharmaceuticals. The use of gas target for the production of short-lived radionuclides such as ^{81}Rb , ^{11}C , ^{15}O , ^{13}N and ^{18}F has become more and more important [4, 9, 10, 12, 17, 20, 23]. One of the main advantages of the use of target chambers filled with an inert gas is the relatively simple separation of the produced radionuclide from the gas. The most important parameter, which should be taken into consideration in designing and fabrication of the gas target, is its capability to assure high beam current. The gas target system basically consists of: (a) collimator; (b) double windows (the first separating the cyclotron vacuum and the second for the target chamber); (c) target gas chamber; (d) an electrically insulated beam stopper.

Production of ^{81}Rb usually involves proton irradiation of natural krypton to utilize the $^{82}\text{Kr}(p,2n)^{81}\text{Rb}$, $^{83}\text{Kr}(p,3n)^{81}\text{Rb}$, $^{84}\text{Kr}(p,4n)^{81}\text{Rb}$ nuclear reactions. $^{81\text{m}}\text{Kr}$ is then obtained from ^{81}Rb through a $^{81}\text{Rb}/^{81\text{m}}\text{Kr}$ generator in which the following reactions take place:



M. R. Aboudzadeh Rovais✉, M. Mirzaii, M. Kiyomarsi, K. Yousefi, N. Shadanpour, M. R. Ensaf
 Agricultural, Medical and Industrial Research School (AMIRS),
 Nuclear Science and Technology Research Institute (NSTRI),
 P. O. Box 31485-498, Karaj, Iran,
 Tel.: +98 261 446 4062, Fax: +98 261 446 4053,
 E-mail: Mraboudzadeh@nrcam.org

Received: 2 June 2008

Accepted: 29 December 2009

Clinical use of the generator has been reported by Jones and Clark [13] and Yano *et al.* [24]. The short-lived radionuclide ^{81m}Kr (13 s), a daughter of ^{81}Rb (4.6 h), has found wide application in routine nuclear medicine for lung ventilation studies. To achieve high density images in a short period of time with low radiation exposure, a relatively large amount of ^{81m}Kr can be used. Furthermore, ^{81}Rb having a metabolic similarity to potassium, is also used to show diagnostic potential.

The characteristics that make ^{81m}Kr attractive as a substitute for ^{133}Xe and ^{99m}Tc for clinical applications are as follows:

1. ^{81m}Kr is an inert gas which is used in scintigraphic examinations.

Table 1. Percent abundance of the stable krypton isotopes in the natural krypton gas

^{78}Kr	^{80}Kr	^{82}Kr	^{83}Kr	^{84}Kr	^{86}Kr
0.35%	2.25%	11.6%	11.5%	57%	17.3%

2. ^{81m}Kr emits only one photon at 190 keV, thus presenting an extremely simple spectral emission.
3. Since ^{81m}Kr has a short physical half-life and short biological half-life, it is possible to administer it with a high activity often required for short studies.
4. It is obtained from a $^{81}\text{Rb}/^{81m}\text{Kr}$ generator which can also be used in medical centers located at a distance from the place where such generators are prepared.

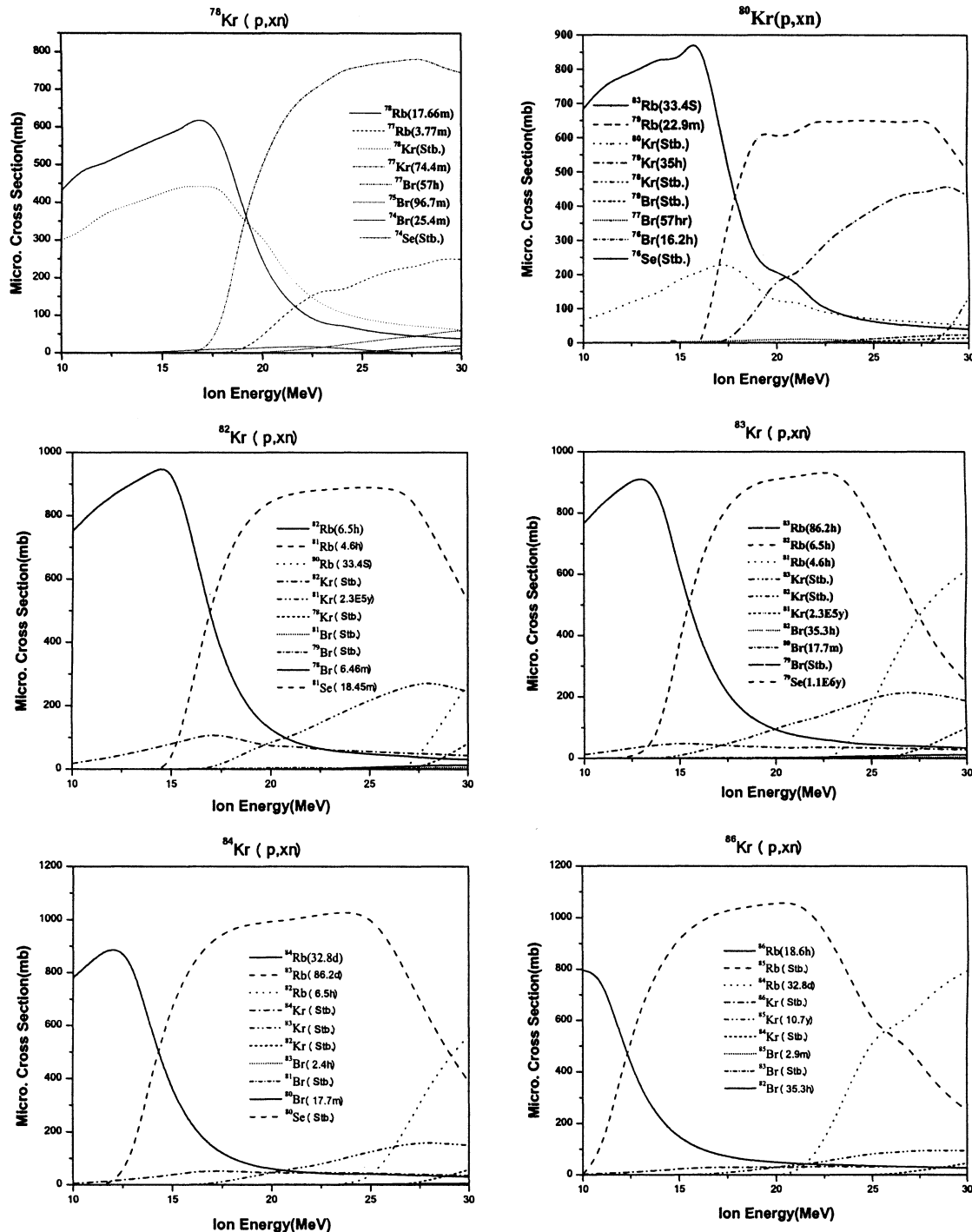


Fig. 1. Excitation functions of $^{nat}\text{Kr}(p,xn)$ simulated by ALICE-91.

The methods most frequently used for ^{81}Rb production are as follows:

1. Bombardment of NaBr or Cu_2Br_2 with α particles up to 35 MeV ($^{79}\text{Br}(\alpha,2n)$) [5, 11, 15].
2. Bombardment of NaBr, Cu_2Br_2 or ^{80}Kr enriched targets with ^3He with energies up to 50 MeV ($^{79}\text{Br}(^3\text{He},n)$, $^{80}\text{Kr}(^3\text{He},pn)$) [11, 20].
3. Bombardment of enriched ^{80}Kr or ^{82}Kr with deuterons with energies up to 52 MeV ($^{80}\text{Kr}(d,n)$, $^{82}\text{Kr}(d,3n)$) [1, 6, 20].
4. Bombardment of natural or enriched Kr, or RbCl, with protons up to 32 MeV and 60 MeV ($^{82}\text{Kr}(p,2n)$, $^{\text{nat}}\text{Rb}(p,xn)$), respectively [1, 7, 8, 14, 16, 18, 19].

Using a 30 MeV cyclotron (Cyclone-30, IBA) at the AMIRS, one of the fields of interest concerns the irradiation of krypton gas with protons for the production of ^{81}Rb . In this paper, the use of nuclear data in targetry of krypton gas target is described.

Theory

Nuclear data

For optimization of a production yield, knowledge of reaction cross-section data is essential. With these data the most suitable energy range for the production of a radionuclide can be determined. Since the natural krypton is a mixture of several isotopes with different abundance (Table 1), the cross-section for the formation of ^{81}Rb from the proton induced nuclear reactions with different isotopes are simulated by using a hybrid model code ALICE-91. The hybrid model code ALICE-91 is a nuclear reaction code which can be used for proton induced reactions [2].

The calculated cross-sections of the $^{\text{nat}}\text{Kr}(p,xn)$ reactions in the energy range of 10–30 MeV are shown in Fig. 1. This figure shows that various other radionuclides can be produced beside ^{81}Rb . These radionuclides can be divided into three groups regarding ^{81}Rb half-life. The first and third groups have half-lives less and more than 4 times of ^{81}Rb half-life, respectively. The two mentioned groups are not important, since they are stable or decay before usage of $^{81}\text{Rb}/^{81\text{m}}\text{Kr}$ generator. The radionuclides that have half-lives near that of ^{81}Rb such as ^{82}Rb (6.5 h) are radionuclidic impurities. The impurities other than Rb radionuclides can be separated by chemical processing such as chromatography and solvent extraction. The Rb radionuclide impurities can be minimized by the optimization of proton energy window in the nuclear reaction. The most important impurity that should be minimized is ^{82}Rb .

The simulated cross-sections for formation of ^{81}Rb and ^{82}Rb by proton induced nuclear reactions on natural krypton are shown in Fig. 2. By analysis of these cross-section curves, the energy range of 26.5–21 MeV was considered to be ideal for production of ^{81}Rb .

Targetry

The target parameters were determined on the basis of nuclear data, commensurate with a high yield of ^{81}Rb and low radionuclidic impurities. Designing of a chamber is

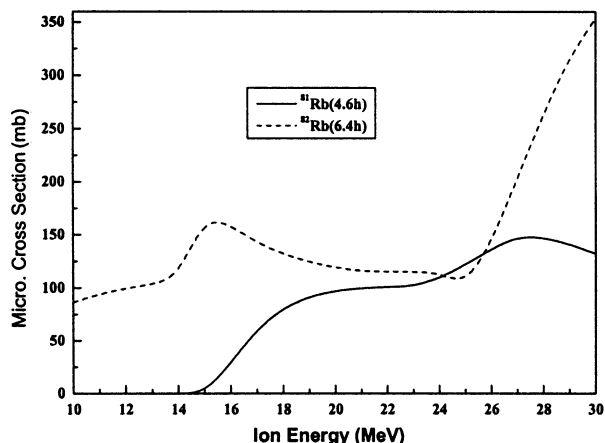


Fig. 2. Simulated excitation functions for formation of ^{81}Rb and ^{82}Rb in proton induced nuclear reactions on natural krypton by ALICE-91.

one of the most important parameters in gas targetry. The chamber's length is a function of the energy range. A selection of the proton energy range that will maximize the yield of the desired product and minimize radionuclidic impurities is of vital importance. Hence, first, the projected range for proton in ideal range of energy should be calculated. The SRIM code calculates the stopping power and range of ions (10 eV–2 GeV/amu) in matter using a full quantum mechanical treatment of ion-atom collisions [25]. Figure 3 shows the simulated stopping range for proton in the energy range of 10–30 MeV on natural krypton.

According to this simulation, the appropriate length of krypton target for reducing proton energy from 26.5 MeV to 21 MeV was 473 mm. The common geometry of gas chamber is conic, because the proton beam itself becomes broader along its path due to scattering. The other advantage of this geometry is the amount of gas required to fill the target, which is less than in cylindrical designs. The dimensions correspond to the beam shape in krypton was calculated by SRIM as a Monte Carlo simulator. Two-dimensional projections of proton on krypton gas target in different planes are shown in Fig. 4.

The SPUTTER.TXT is one of the data files that is stored by running the SRIM code. These data file

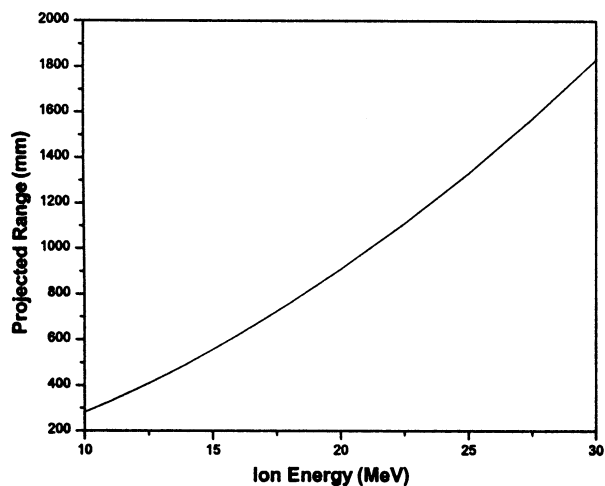


Fig. 3. Projected range of proton on natural krypton gas (2.5 atm and 25°C).

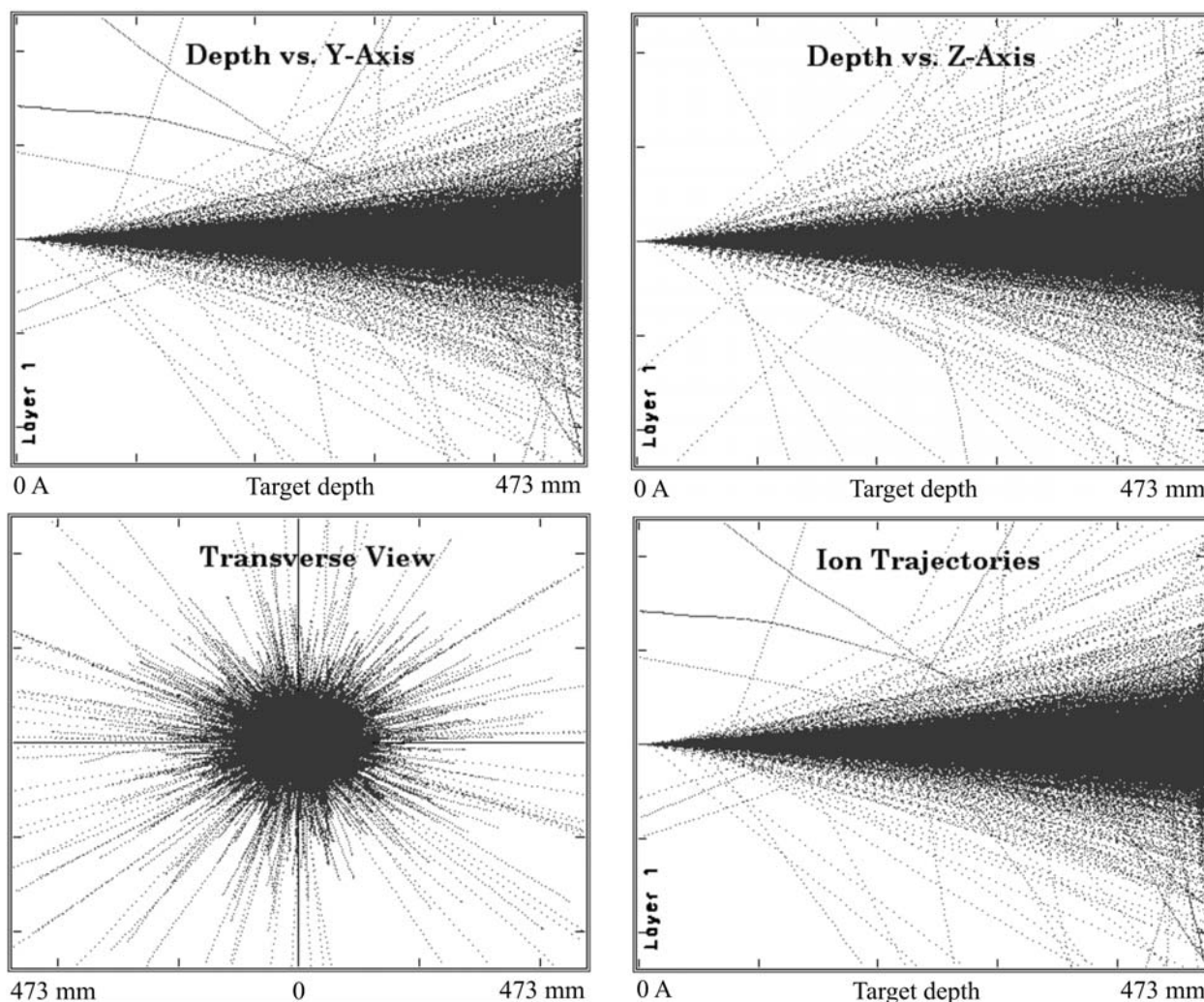


Fig. 4. Simulated two-dimensional projection of protons on krypton gas (2.5 atm and 25°C). The coordinate system of SRIM is defined as the X-axis, being the depth into the target, and the Y-axis and the Z-axis being transverse.

include the protons final trajectory and energy that may be analyzed to find the divergent angle of protons in krypton. By considering the maximum number of collisions between the proton and krypton and the minimum dead volumes in target design, the optimized divergent angle for the cone was found to be at 2.4 degree.

Selection of the right material is another important parameter in targetry. Gas temperature will increase during the irradiation as the protons lose their energy in the gas target. In order to control the gas temperature, the target material has to be a good heat conductor and also easily available. Materials such as copper, aluminum or stainless steel are preferred. The heat conductivity of stainless steel is not as good as that of aluminum or copper. The disadvantages of copper are rapid oxidation when heated in air, and a high coefficient of thermal expansion. A target body of aluminum was initially considered appropriate because:

1. The raw materials used were available locally.
2. Since the radionuclides produced through proton bombardment on aluminum are short-lived, the personnel radiation exposure is reduced during target maintenance.
3. Ease of machining.
4. Proper thermal conductivity (250 W/m·K).

Several laboratories, however, have adopted an aluminum target chamber and met the following problems [16, 21, 22]:

1. The recovery yield of ^{81}Rb was diminished with repeated usage.
2. Corrosion of the target body and window foil.
3. Elution of metallic impurities along with ^{81}Rb (possible chemical forms for this precipitate include $\text{AlO}(\text{OH})$ and $\text{Al}(\text{OH})_3$).

Since the stainless steel is resistant against elution, corrosion and rapid oxidation, it was selected to be the proper material for the target body.

Yield

The yield of a radionuclide expected from a particular thickness of the target (thick target yield) can be calculated by integration of an experimentally determined or theoretically estimated excitation function over the energy range covered by the target. The calculated yield, however, represents the maximum yield which can be expected via a given nuclear process. In practice, the experimental yields are usually lower than the theoretical values.

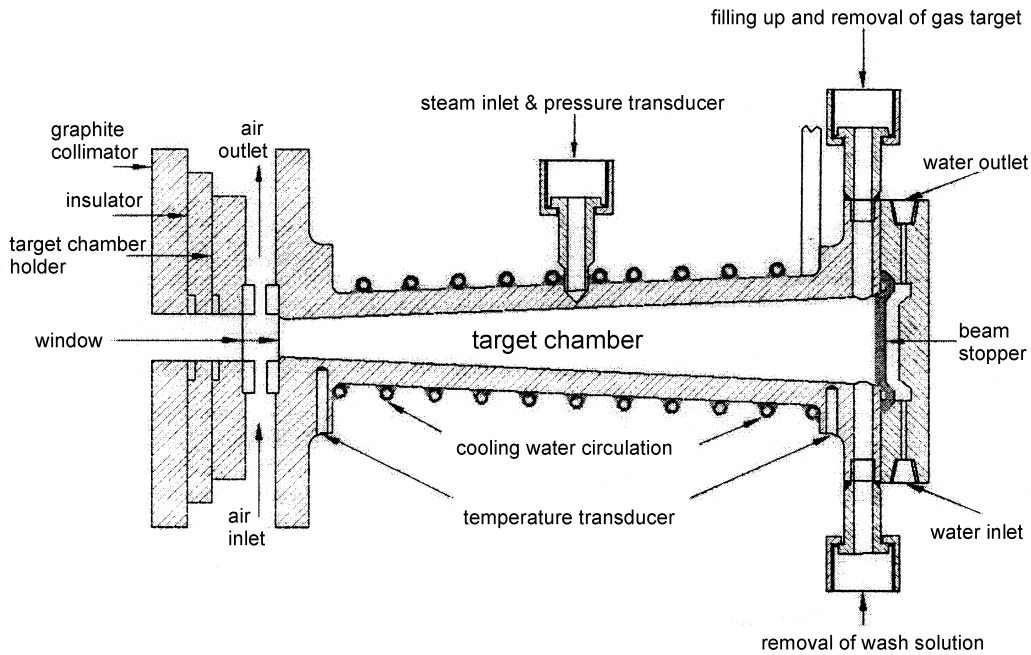


Fig. 5. Conically shaped gas target system with double window air cooling in the front and water cooling of the target body. The dimensions correspond to the beam shape, which was calculated by SRIM.

The theoretical production yield of $^{nat}\text{Kr}(p,xn)^{81}\text{Rb}$ can be calculated by:

$$(2) \quad R = \int_0^L \frac{\delta(x) \times n \times I \times 3600 \times \left(1 - e^{\left(\frac{-0.693}{T_{1/2}}\right)t}\right)}{3.7 \times 10^7} dx$$

where: R – production yield ($\text{mCi}/\mu\text{A}\cdot\text{h}$); L – length of target (mm); $\delta(x)$ – reaction cross-section at particle energy (cm^2); n – number of atoms per volume (no/cm^3); I – proton beam current on target in μA ; $T_{1/2}$ – product half-life (s); dx – physical thickness (mm).

Experimental

The estimated target length was reduced to 251 mm due to limitation of the facility in our workshop. The conical target designed for the production of ^{81}Rb via the $^{nat}\text{Kr}(p,xn)^{81}\text{Rb}$ using 26.5 MeV protons is shown in Fig. 5. The stainless steel target chamber has a conical shape with front and back diameters of 17 and 38 mm, respectively. The target front is equipped with double $20 \mu\text{m}$ titanium windows which are cooled by air and the stainless steel tubes which are welded to the target body for circulating cooling water.

Water circulating around the target body provides cooling during the irradiation time to 295 K. All irradiations were performed at the AMIRS 30 MeV cyclotron using a focused 26.5 MeV proton beam. The beam current was monitored by an ammeter during the irradiation.

A schematic representation of the production system is given in Fig. 6. In general, the production cycle consisted of the following operations:

1. Setting of a proper vacuum (about 10^{-5} mbar).
2. Filling of the target with natural krypton to 2.5 atm (safety of operating at a relatively low pressure is

high because it significantly reduces the stress and mechanical shock on the target window).

3. Starting of the cooling system.
4. Irradiation of the gas target.
5. Recovery of the krypton gas via a cryogenic vessel after the end of bombardment.
6. Washing of the target walls via introduction of steam (the rubidium adsorbed on the walls of chamber was dissolved).
7. Collection of condensed water containing radionuclides of rubidium.

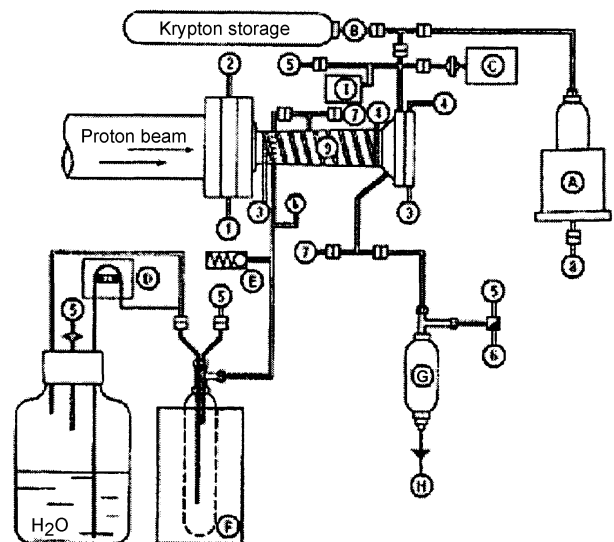


Fig. 6. Schematic representation of ^{81}Rb production system. 1 – air inlet for window cooling; 2 – air outlet; 3 – water inlet for target cooling; 4 – water outlet; 5 – atmosphere; 6 – pressurized air; 7 – vacuum line; 8 – liquid nitrogen; 9 – target body. A – main cryogenic trap; B – secondary cryogenic trap; C – vacuum gauge; D – peristaltic pump; E – safety valve; F – steam oven; G – collection vessel; H – transfer tubing; I – target pressure gauge.

Table 2. Practical yield at the end of bombardment of target for different test runs^a

Test no	1	2	3	4	5
Practical yield (mCi/ μ A·h)	2.73	3.19	3.24	3.36	3.40
Average practical yield (mCi/ μ A·h)	3.18	3.18	3.18	3.18	3.18
Standard deviation	0.27	0.27	0.27	0.27	0.27

^aTheoretical yield: 4.1 mCi/ μ A·h.

8. Transfer of the aqueous solution to a receiving vessel located in a hot cell.
9. The qualified samples were allocated for loading of the generators.
10. For loading of the generators on demand activity, a specified volume of the ⁸¹Rb solution was purged by passing through a special ion exchanger which was fitted into a transportable lead shield for trapping ⁸¹Rb. To be able to make use of the whole krypton gas deposited in the storage vessel, an intermediary krypton trap was inserted in the filling circuit. The small volume of a liquid nitrogen cooled stainless steel finger to allow temporarily trapping of all the krypton gas from the storage vessel and the chamber of target.

In this production system, the steam was generated by a steam oven and the collected washing solution was pneumatically transferred to the chemical processing area for converting into their final form in a hot cell. The radionuclidic quality control of the product was achieved by an HPGe detector.

Results and discussion

Gas target systems have certain unique advantages, as well as some disadvantages, for preparation of radio-pharmaceuticals. The current production target system for preparation of the ⁸¹Rb/^{81m}Kr generator allows easily loading and unloading of the target as well as processing of the radionuclide through remote operation. However, utilization of this production target chamber has necessitated elevated gas pressures which require entrance window thickness sufficient to withstand the differential pressure. Therefore, the windows were selected from titanium foil with a thickness of 20 μ m.

Several test runs were performed to check the target design. The theoretical yields and the practical yields were compared. The proton energy and the beam current were chosen to be 26.5 MeV and 10 μ A, respectively. It was calculated that the incident beam energy is degraded to around 25.7 MeV by the double titanium foils and about 3 MeV is dropped in the gas, with 22.7 MeV in the beam stopper. Table 2 summarizes the results of the practical yields obtained from different tests.

The average of the practical yield (3.18 mCi/ μ A·h) for the 251 mm long gas target corresponded to more than 80% of the theoretical value (4.1 mCi/ μ A·h) that was calculated by Eq. (2). This theoretical yield was calculated using the obtained cross-section values from the ALICE-91 code. Disagreement between the theoretical and practical yields can be attributed to the following factors:

1. There are some simplified assumptions in ALICE-91 code [3], which have to be taken into account. For example, in hybrid models [2], which is proposed by

M. Blann, it is assumed that the partial input waves in emission probability PE (pre-equilibrium) which is $P_v(\epsilon)$ does not effect the outcome. This assumption is based on the theory that the nucleus has a homogeneous nucleus material, where in practice, it is not the case.

2. The energy loss of protons in krypton gas was obtained from the simulation results by SRIM code in which also there are simplified assumptions.
3. Large volume of gas targets introduces a degree of uncertainty for an absolute measurement of the ⁸¹Rb activity caused by degradation and straggling of the beam. Scattering effects may significantly increase, as a result of the increased target pressure. Moreover, thermal changes resulting from particles energy degradation within the target gas will contribute to the reduction in gas density within the target region traversed by the beam.
4. The inside chamber surface is not perfectly smooth; hence, part of the produced Rb could be trapped by the roughness of the surface which needs more investigation.

The production yield of ⁸¹Rb can be enhanced by using isotopically enriched ⁸²Kr. The designed target is being used for routine production of ⁸¹Rb/^{81m}Kr generators and covers the local demands.

References

1. Acerbi E, Birattari C, Bonardi M, De Martinis C, Salomone A (1981) Kr(p,xn) excitation functions and ⁸¹Rb(^{81m}Kr) generator studies. *Int J Appl Radiat Isot* 32:465–475
2. Blann N (1987) Calculation of excitation functions with code ALICE. In: Proc of the IAEA consultants' meeting on data requests for medical radioisotope production, 20–24 April 1987, Tokyo, Japan. IAEA, Vienna, pp 20–24
3. Buthelezi EZ, Nortier FM, Schroeder IW (2006) Excitation functions for the production of ⁸²Sr by proton bombardment of ^{nat}Rb at energies up to 100 MeV. *Appl Radiat Isot* 64:8:915–924
4. Firouzbakht ML, Schlyer DJ, Fowler JS (1999) Cryogenic target design considerations for the production of [¹⁸F] fluoride from enriched [¹⁸O]carbon dioxide. *Nucl Med Biol* 26:749–753
5. Fremlin JH, Stammers K, Stewart FR (1978) A new generator for krypton-81m. *Nucl Instrum Methods* 156:369–373
6. Gindler JE, Oselka MC, Friedman AM, Mayron LW, Kaplan E (1976) A gas target assembly for the production of high purity, high specific activity ⁸¹Rb. *Int J Appl Radiat Isot* 27:330–332
7. Guillaume M, Brihaye C (1987) Generators of ultra short lived radionuclide for routine clinical applications. *Radiochim Acta* 41:119–130
8. Hammond RG, Renton ML, Mackay DB, Waters SL (1997) Design and operation of a krypton-82 gas target for the regular high yield production of rubidium-81 for

- the preparation of krypton-81m generators. In: Proc of the 7th Int Workshop on Targetry and Target Chemistry, 8–11 June 1997, Heidelberg, Germany, pp 51–55
9. Heselius SJ, Malmberg P, Solin O, Långström B (1987) Studies of proton beam penetration in nitrogen-gas target with respect to production and specific radioactivity of Carbon-11. *Appl Radiat Isot* 38:49–57
 10. Hess E, Blessing G, Coenen HH, Qaim SM (2000) Improved target system for production of high purity [^{18}F] fluorine via the $^{18}\text{O}(\text{p},\text{n})^{18}\text{F}$ reaction. *Appl Radiat Isot* 52:1431–1440
 11. Homma Y, Kurata K (1979) Excitation functions for the production of ^{81}Rb ($^{81\text{m}}\text{Kr}$) via the $^{79}\text{Br}(\alpha,2\text{n})^{81}\text{Rb}$ and the $^{81}\text{Br}(\text{He},2\text{n})^{81}\text{Rb}$ reaction. *Int J Appl Radiat Isot* 30:345–348
 12. Hur MG, Kim SW, Yang SD *et al.* (2007) Design of a tandem target for a simultaneous production of C-11 and F-18 with 18 MeV. *Nucl Instrum Methods B* 261:800–802
 13. Jones T, Clark JC (1969) A cyclotron produced ^{81}Rb - $^{81\text{m}}\text{Kr}$ generator and its use in γ camera studies. *Br J Radiol* 42:237–238
 14. Kovacs Z, Tarkanyi F, Qaim SM, Stöcklin G (1991) Excitation functions for the formation of some radioisotopes of rubidium in proton induced nuclear reactions on Kr-nat, Kr-82 and Kr-83 with special reference to the production of Rb-81 ($^{81\text{m}}\text{Kr}$) generator radionuclide. *Appl Radiat Isot* 42:329–335
 15. Moroji T, Lambrecht RM, Wolf AP, Thakur ML (1980) Cyclotron isotopes and radiopharmaceuticals – XXX. Aspects of production, elution and automation of $^{81}\text{Rb}/^{81\text{m}}\text{Kr}$ generators. *Int J Appl Radiat Isot* 31:1:51–59
 16. Mulders JJJ (1984) Yield curves and beam current dependent production rates of Rb radioisotopes produced by protons on a krypton gas target. *Int J Appl Radiat Isot* 35:475–480
 17. Powell J, O'Neil JP (2006) Production of [^{15}O]water at low-energy proton cyclotrons. *Appl Radiat Isot* 64:755–759
 18. Schnei RJ, Goldb CJ (1976) Production of rubidium-81 by the reaction $^{85}\text{Rb}(\text{p},5\text{n})^{81}\text{Sr}$ and decay of ^{81}Sr . *Int J Appl Radiat Isot* 27:189–191
 19. Solin O, Heselius SJ, Lindblom P, Mangard PJ (1984) Production of ^{81}Rb from Kr – a target study. *J Labelled Compd Radiopharm* 21:1275–1277
 20. Uhlir V, Gasper H, Helus F (1996) A new ^{81}Rb - $^{81\text{m}}\text{Kr}$ generator from enriched ^{82}Kr gas for medical use. *J Radioanal Nucl Chem* 204:423–427
 21. Vandecasteele C, Goethals P, Sambre J, Slegers G (1981) Routine production of ^{81}Rb - $^{81\text{m}}\text{Kr}$ generators using the $^{81}\text{Kr}(\text{p},2\text{n})^{81}\text{Rb}$ reaction. *Radiochem Radio* 46:5:285–290
 22. Waters SL, Clark JC, Harlock PL, Brown C, Bett R, Sims HE (1986) Production of ^{81}Rb using 60 MeV proton beam. Target development and aspect of recovery. *J Labelled Compd Radiopharm* 23:314–316
 23. Yang SD, Kim SW, Hur MG, Park JH, Chai JS, Yu KH (2007) Design and evaluation of tandem target for a simultaneous production of [^{11}C]CH₄ and [^{18}F]-fluoride. *Nucl Med Biol* 34:117–120
 24. Yano Y, MacRae J, Anger HO (1970) Lung function studies using short-lived $^{81\text{m}}\text{Kr}$ and the scintillation camera. *J Nucl Med* 11:674–679
 25. Ziegler JF, Biersack JP, Littmark U (1985) The stopping and range of ions in solids. Pergamon Press, New York